

RESEARCH ARTICLE | FEBRUARY 02 2023

## Fast crystallization below the glass transition temperature in hyperquenched systems

Special Collection: [Nucleation: Current Understanding Approaching 150 Years After Gibbs](#)

Pierre Lucas   ; Wataru Takeda  ; Julian Pries  ; Julia Benke-Jacob; Matthias Wuttig 



*J. Chem. Phys.* 158, 054502 (2023)

<https://doi.org/10.1063/5.0136306>

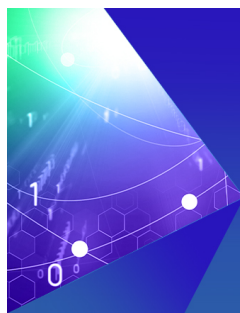


View  
Online



Export  
Citation

CrossMark



Chemical Physics Reviews

Special Topic: Molecular Approaches  
for Spin-based Technologies

Submit Today!

# Fast crystallization below the glass transition temperature in hyperquenched systems

Cite as: J. Chem. Phys. 158, 054502 (2023); doi: 10.1063/5.0136306

Submitted: 25 November 2022 • Accepted: 15 January 2023 •

Published Online: 2 February 2023



Pierre Lucas,<sup>1,a)</sup> Wataru Takeda,<sup>1</sup> Julian Pries,<sup>2</sup> Julia Benke-Jacob,<sup>2</sup> and Matthias Wuttig<sup>2,3</sup>

## AFFILIATIONS

<sup>1</sup> Department of Materials Science and Engineering, University of Arizona, Tucson, Arizona 85712, USA

<sup>2</sup> Institute of Physics IA, RWTH Aachen University, 52074 Aachen, Germany

<sup>3</sup> Peter Grünberg Institute (PGI 10), Forschungszentrum Jülich, 52428 Jülich, Germany

**Note:** This paper is part of the JCP Special Topic on Nucleation: Current Understanding Approaching 150 Years After Gibbs.

**a)** Author to whom correspondence should be addressed: [Pierre@arizona.edu](mailto:Pierre@arizona.edu)

## ABSTRACT

Many phase change materials (PCMs) are found to crystallize without exhibiting a glass transition endotherm upon reheating. In this paper, we review experimental evidence revealing that these PCMs and likely other hyperquenched molecular and metallic systems can crystallize from the glassy state when reheated at a standard rate. Among these evidences, PCMs annealed below the glass transition temperature  $T_g$  exhibit slower crystallization kinetics despite an increase in the number of sub-critical nuclei that should promote the crystallization speed. Flash calorimetry uncovers the glass transition endotherm hidden by crystallization and reveals a distinct change in kinetics when crystallization switches from the glassy to the supercooled liquid state. The resulting  $T_g$  value also rationalizes the presence of the pre- $T_g$  relaxation exotherm ubiquitous of hyperquenched systems. Finally, the shift in crystallization temperature during annealing exhibits a non-exponential decay that is characteristic of structural relaxation in the glass. Modeling using a modified Turnbull equation for nucleation rate supports the existence of sub- $T_g$  fast crystallization and emphasizes the benefit of a fragile-to-strong transition for PCM applications due to a reduction in crystallization at low temperature (improved data retention) and increasing its speed at high temperature (faster computing).

Published under an exclusive license by AIP Publishing. <https://doi.org/10.1063/5.0136306>

## INTRODUCTION

Crystallization below the glass transition temperature  $T_g$  is normally extremely slow due to the kinetically arrested atomic mobility in this temperature range.<sup>1</sup> Although oxide glasses mainly obey this behavior, organic glasses commonly exhibit unusually high crystallization rates below  $T_g$ .<sup>2–9</sup> This behavior results from a decoupling between crystallization rates and viscous flow caused by interfacial effects. Hikima *et al.*<sup>2</sup> observed anomalously high crystallization rates in the glass transition region of *o*-terphenyl and assigned it to an enhancement of homogeneous nucleation at the liquid–crystal interface. A similar process was observed by Ishida *et al.* in nifedipine.<sup>3</sup> Schammé *et al.* assigned the crystallization of ball-milled quinidine amorphous powders to high molecular mobility on the surface of amorphous grains.<sup>4</sup> Willart *et al.* observed an identical effect in griseofulvin.<sup>5</sup> Yu *et al.* also observed fast surface crystallization and glass-crystal growth in several organic compounds.<sup>6–9</sup> Although the crystallization rate of these systems is abnormally high in the region

directly below  $T_g$  due to decoupling from viscosity, they are relatively good glass-formers, and all exhibit a clear calorimetric glass transition. Instead, an increasing number of rapidly quenched systems have been found to crystallize prior to exhibiting a calorimetric glass transition: this includes water,<sup>10,11</sup> metallic glasses,<sup>12,13</sup> and phase change materials (PCMs).<sup>14–16</sup> In these systems, rapid crystallization occurs at temperatures up to 50 °C below  $T_g$  where diffusive processes would normally be exceedingly slow. The inability to observe a clear glass transition has in some cases led to controversies such as in the case of water.<sup>10,17,18</sup> Here, we review experimental evidences indicating that fast sub- $T_g$  crystallization occurs in many amorphous PCMs. Then, we use the Turnbull method to explain the phenomenon and its relation to fragility.

## SUB- $T_g$ CRYSTALLIZATION IN PCMs

PCMs exhibit a range of crystallization behavior depending on their composition.<sup>19</sup> Prominent PCMs such as  $\text{Ge}_2\text{Sb}_2\text{Te}_5$ ,

AIST ( $\text{Ag}_4\text{In}_3\text{Sb}_{67}\text{Te}_{26}$ ), or GeTe all crystallize without prior glass transition endotherms when reheated at conventional rates ( $\sim 20^\circ\text{C}/\text{min}$ ).<sup>14–16</sup> Other PCMs such as  $\text{Ge}_3\text{Sb}_6\text{Te}_5$  exhibit a clear glass transition prior to crystallization.<sup>20</sup> Figure 1 compares the excess heat capacity  $C_p^{\text{exc}}$  of as-deposited GeTe and  $\text{Ge}_3\text{Sb}_6\text{Te}_5$  during a heating ramp at a rate of  $40^\circ\text{C}/\text{min}$ . The comparison of these two glasses is insightful because they have nearly identical  $T_g$  values, i.e.,  $T_g = 190^\circ\text{C}$  for GeTe<sup>16</sup> and  $T_g = 193^\circ\text{C}$  for  $\text{Ge}_3\text{Sb}_6\text{Te}_5$ <sup>20</sup> but exhibit distinct crystallization behavior. The first feature on the thermogram of Fig. 1 is an exotherm starting near  $100^\circ\text{C}$ , which is characteristic of hyperquenched systems trapped in a high fictive temperature state.<sup>21</sup> During reheating at a slow rate, both glasses release enthalpy as they dynamically relax toward the metastable supercooled liquid state.  $\text{Ge}_3\text{Sb}_6\text{Te}_5$  eventually exhibits a glass transition endotherm near  $193^\circ\text{C}$  prior to crystallization near  $230^\circ\text{C}$ . In contrast, GeTe starts to crystallize as it is still relaxing tens of degrees below  $T_g$ . This strongly suggests that GeTe (and other PCMs) crystallizes from the glassy state instead of the supercooled liquid state above  $T_g$ .

The absence of a clear calorimetric glass transition endotherm in some PCMs has led to a broad range of reported  $T_g$  values spanning in some cases over  $100^\circ\text{C}$ .<sup>22–26</sup> For example,  $T_g$  values for  $\text{Ge}_2\text{Sb}_2\text{Te}_5$  have been reported from  $100^\circ\text{C}$ <sup>22</sup> to  $200^\circ\text{C}$ <sup>26</sup> and that of AIST from  $105^\circ\text{C}$ <sup>27</sup> to  $182^\circ\text{C}$ .<sup>15</sup> However,  $T_g$  of PCMs can also be estimated from their relaxation exotherm using the Velikov *et al.* method,<sup>11</sup> as shown in Fig. 2. It is found that hyperquenched glasses spanning many categories of compositions (metallic, oxides, covalent, organic), a broad range of fragility ( $m = 17–81$ ), and a broad range of  $T_g$  ( $-30$  to  $670^\circ\text{C}$ ) all obey a similar pattern of exothermic relaxation when reheated at a slow rate. All systems exhibit a maximum in relaxation of trapped enthalpy near  $T/T_g \approx 0.9$ . This provides an alternative mean of estimating  $T_g$  for controversial PCMs such as  $\text{Ge}_2\text{Sb}_2\text{Te}_5$ . A  $T_g$  assignment of  $200^\circ\text{C}$  for  $\text{Ge}_2\text{Sb}_2\text{Te}_5$  shows a relaxation behavior consistent with all systems and, in

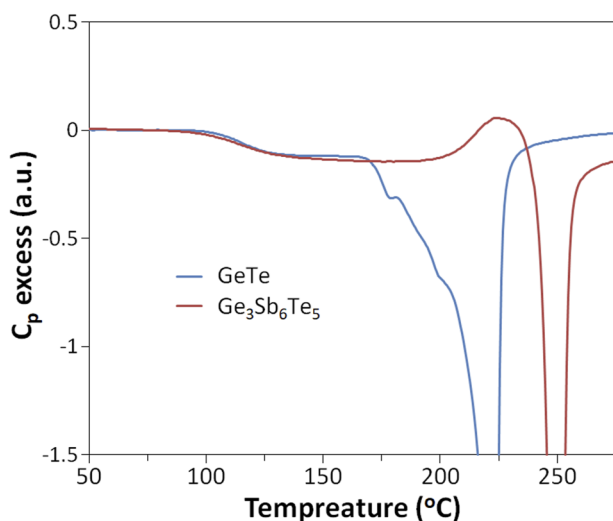


FIG. 1. Excess heat capacity  $C_p^{\text{exc}}$  of as-deposited GeTe and  $\text{Ge}_3\text{Sb}_6\text{Te}_5$  during a heating ramp at a rate of  $40^\circ\text{C}/\text{min}$  (data from Refs. 16 and 20).

particular, with that  $\text{Ge}_3\text{Sb}_6\text{Te}_5$ , where  $T_g$  is unambiguously known. Instead, a  $T_g$  assignment of  $110^\circ\text{C}$  indicates a glass that would undergo a maximum relaxation at a temperature above  $T_g$  when the system has already reached the supercooled liquid. This outcome is not sound since there would be no driving force for relaxation in the metastable supercooled liquid state. The  $T_g$  must, therefore, lay at higher values. The same pattern is observed for GeTe with a  $T_g = 193^\circ\text{C}$  and AIST with a  $T_g = 182.5^\circ\text{C}$ . In turn, this indicates that these PCMs, indeed, crystallize below  $T_g$  as previously reported.<sup>14–16</sup>

Further evidence for sub- $T_g$  crystallization in PCMs can be garnered through the use of flash differential scanning calorimetry (FDSC).<sup>14,15</sup> As shown by Henderson,<sup>34</sup> the application of the Kissinger method<sup>35</sup> to crystallization kinetics indicates that the temperature of a crystallization exotherm maximum  $T_P$  is a function of the heating rate due to the kinetic barrier for crystal growth in the supercooled liquid. Specifically, higher heating rates permit to delay the crystallization event to higher temperatures. Then, the use of FDSC should permit to notably raise the onset of the crystallization exotherm. This offers a strategy to uncover the glass transition endotherm that is hidden by crystallization at standard heating rates. Figure 3(a) shows the thermograms obtained from heating as-deposited  $\text{Ge}_2\text{Sb}_2\text{Te}_5$  at rates ranging from 50 K/s to 30 000 K/s. At slower rates, the relaxation exotherm is present prior to crystallization along with the evolution of the so-called “shadow-glass transition.”<sup>18</sup> At sufficiently high rates near 10 000 K/s, the relaxation exotherm vanishes and reveals a glass transition endotherm

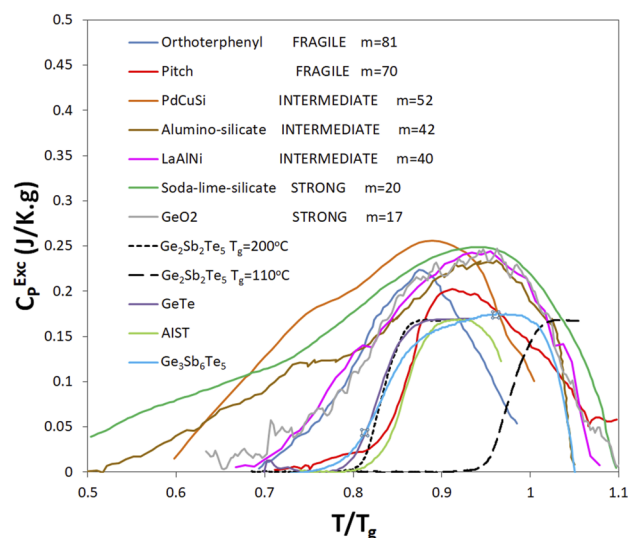
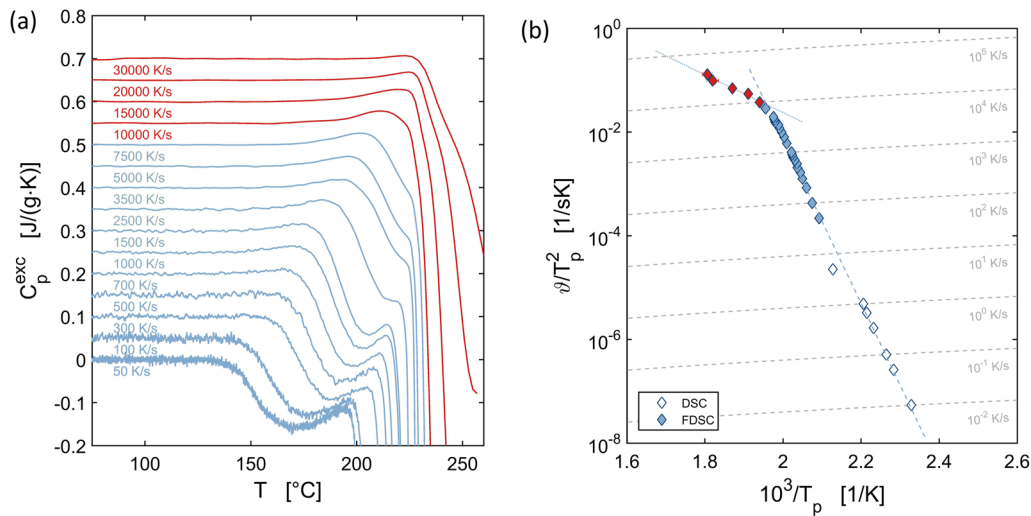


FIG. 2. Enthalpy recovery exotherm for a wide variety of hyperquenched glasses including oxide, metallic, and molecular glasses over a broad range of  $T_g$  ( $-30$  to  $670^\circ\text{C}$ ) and a broad range of fragility ( $m = 17–81$ ). Orthoterphenyl,<sup>11</sup> Pitch,<sup>28</sup>  $\text{Pd}_{77.5}\text{Cu}_6\text{Si}_{16.5}$ ,<sup>29</sup>  $\text{La}_{55}\text{Al}_{25}\text{Ni}_{20}$ ,<sup>30</sup> Basaltic fiber ( $\text{SiO}_2$  49.3  $\text{Al}_2\text{O}_3$  1.8  $\text{FeO}$  11.7  $\text{CaO}$  10.4  $\text{MgO}$  3.9  $\text{Na}_2\text{O}$  3.9  $\text{K}_2\text{O}$  0.7),<sup>31</sup> soda-lime-silicate ( $\text{SiO}_2$  70.5  $\text{Na}_2\text{O}$  8.7  $\text{K}_2\text{O}$  7.7  $\text{CaO}$  11.6  $\text{Sb}_2\text{O}_3$  1.1  $\text{SO}_3$  0.2),<sup>32</sup> and  $\text{GeO}_2$ .<sup>33</sup> All glasses show the onset of relaxation of trapped enthalpy near  $T/T_g \approx 0.5–0.7$  and a maximum of relaxation near  $T/T_g \approx 0.9$ . Comparison of these exotherms with that of phase change materials using Velikov's excess heat capacity method<sup>11</sup> indicates that the standard  $T_g$  value for  $\text{Ge}_2\text{Sb}_2\text{Te}_5$  is  $\sim 200^\circ\text{C}$ .



**FIG. 3.** (a) Excess heat capacity thermograms of as-deposited  $\text{Ge}_2\text{Sb}_2\text{Te}_5$  obtained by Flash-DSC at a rate spanning 50 to 30 000 K/s. (b) Kissinger plot for as-deposited  $\text{Ge}_2\text{Sb}_2\text{Te}_5$  showing a sudden change in crystallization activation energy from 3.13 eV at low rates to 0.69 eV at high rates (data from Ref. 14).

prior to crystallization. This indicates that the crystallization now takes place from the undercooled liquid rather than the glassy state. If this is the case, the crystallization kinetics should be notably different. The activation energy for crystallization can be obtained through the construction of a Kissinger plot, as shown in Fig. 3(b). The Kissinger plot of  $\text{Ge}_2\text{Sb}_2\text{Te}_5$  shows a sudden change in crystallization activation energy from 3.13 eV (blue markers) to 0.69 eV (red markers) that is concomitant with the switch in crystallization from the glassy state to the supercooled liquid state [Fig. 3(a)].<sup>14</sup> This switch in kinetic behavior was observed for both AIST<sup>15</sup> and  $\text{Ge}_2\text{Sb}_2\text{Te}_5$ .<sup>14</sup> Although the activation energy should be greater in the supercooled liquid than in the glass for standard conditions, numerical simulations show that the decrease in activation energy is the consequence of probing a very fragile system with heating rates high enough to probe the high-temperature region of the fragile liquid where the activation energy becomes lower than that of the glass.<sup>14</sup> This provides additional evidence that these PCMs, indeed, crystallize below  $T_g$ .

It has been previously suggested that fast crystallization of PCMs cannot occur below the standard  $T_g$  due to the kinetic arrest characteristic of this temperature range.<sup>24</sup> In the following, we use the simple kinetic model developed by Turnbull<sup>36</sup> to show that hyperquenching and high fragility of PCMs drastically affect the crystallization kinetics and suggest that fast crystallization can occur below  $T_g$  directly from the glassy state.

## KINETIC MODEL FOR CRYSTALLIZATION IN HYPERQUENCHED SYSTEMS

### Turnbull parameter

In his seminal paper on glass formation,<sup>36</sup> Turnbull derived the reduced glass temperature  $T_{rg} = T_g/T_m$  as a predictive metric for the ability of a system to bypass crystallization and form glass upon

cooling. It was found that systems exhibiting  $T_{rg} > 2/3$  have exceedingly low nucleation rate  $I$  and can easily form a glass. For example,  $T_{rg} = 0.75$  for  $\text{SiO}_2$ , where nucleation is never observed experimentally upon cooling. Conversely, phase change materials are notoriously bad glass-formers and exhibit lower Turnbull parameters, i.e.,  $T_{rg} = 0.46$  for  $\text{GeTe}$ .<sup>16</sup> These predictions are based on the estimation of the temperature dependence of the nucleation rate, as shown in Fig. 4. These estimates result from the balance between the work required to overcome surface tension and the gain in free energy resulting from the growth of the nuclei. Nuclei reaching a critical radius  $r_i$  achieve that balance and can grow further due to an overall decrease in free energy. The growth of these critical nuclei proceeds from the addition of atoms through a diffusion mechanism. The process of transport across the nucleus–matrix interface is controlled by a free energy of activation  $\Delta G'$  and described by a diffusion coefficient  $D$  according to

$$D = D_0 \exp\left(\frac{-\Delta G'}{kT}\right), \quad (1)$$

where  $D_0$  is a constant,  $T$  is the temperature, and  $k$  is Boltzmann's constant. This constitutes the kinetic barrier to nucleation. Then, the diffusion coefficient is related to the viscosity  $\eta$  using the Stokes–Einstein equation

$$D = \frac{kT}{3\pi a_0 \eta}, \quad (2)$$

where  $a_0$  is the diameter of the diffusing species, and  $\eta$  is the viscosity. Following the classical nucleation theory<sup>37</sup> (CNT), the nucleation rate can then be expressed as<sup>36</sup>

$$I = \frac{k_n}{\eta} \exp\left[-\frac{16\pi\alpha^3\beta}{3T_r(\Delta T_r)^2}\right], \quad (3)$$

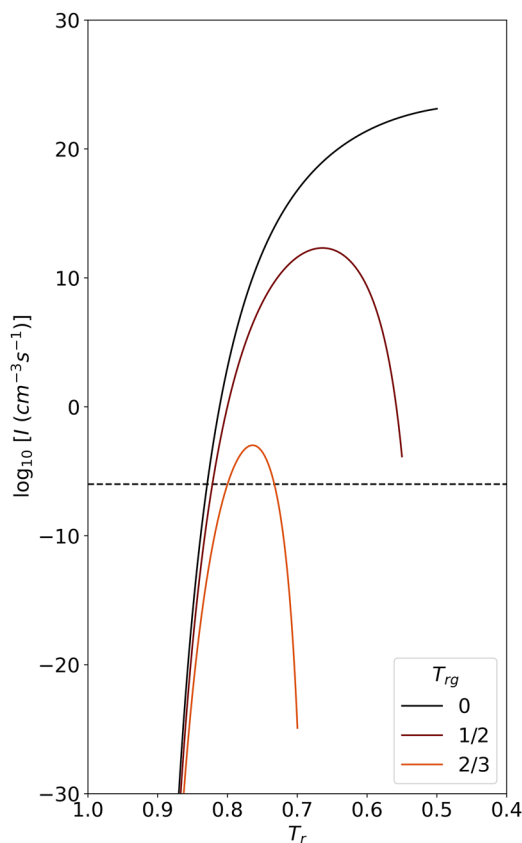


**FIG. 4.** Estimation of the temperature dependence of the nucleation rates  $I$  using the Turnbull method for systems with different reduced glass temperature  $T_{rg}$ . Reproduced from Ref. 36.

where the reduced temperature  $T_r = T/T_m$ , the reduced undercooling  $\Delta T = (T_m - T)/T_m$ ,  $k_n$  is a constant,  $\alpha$  is a dimensionless parameter related to the surface tension, and  $\beta$  is a dimensionless parameter related to the entropy of melting. For small undercooling ( $\Delta T_r \sim 0$ ), the exponent term dominates and  $I$  vanishes, while for large undercooling, the pre-exponent dominates due to the increase in equilibrium viscosity  $\eta$  (following the Vogel–Fulcher–Tammann (VFT) equation), and  $I$  vanishes again. At intermediate temperatures,  $I$  reaches large values that depends on the reduced glass temperature (Fig. 4) as the equilibrium viscosity  $\eta$  is lower, the lower the reduced glass transition temperature  $T_{rg}$ .

The Turnbull model was developed based on the assumption that crystallites form in the undercooled liquid; however, recent observations on poor glass-forming systems shown in the section titled “Sub- $T_g$  Crystallization in PCMs” suggest that crystallization may also take place rapidly from the glassy state. In this case, the characteristic relaxation time that controls viscosity and diffusion should be determined by the isostructural viscosity rather than the equilibrium viscosity. This, in turn, should notably affect estimations of the nucleation rates at large undercooling. Moreover, these relaxation times are a function of temperature, time, as well as quenching rate (i.e., fictive temperature  $T_f$ ) and should affect crys-

tallization kinetics accordingly as described in the next section titled “Relaxation times.”

## Relaxation times

The viscosity  $\eta$  is related to the stress relaxation time  $\tau_s$  according to the Maxwell equation,

$$\eta = G_\infty \tau_s, \quad (4)$$

where  $G_\infty$  is the instantaneous shear modulus, and  $\tau_s$  represents the time constant for the system to respond to a mechanical stress at a given temperature (i.e., beam bending, indentation, parallel plate, rotating cup, and capillary). Measurements performed in the stable liquid above  $T_m$  or the metastable undercooled liquid below  $T_m$  yield the equilibrium stress relaxation time  $\tau_{S(\text{equ})}$ , which increases exponentially with decreasing temperature, as depicted schematically in Fig. 5. Upon cooling at a standard rate of  $\sim 20^\circ\text{C}/\text{min}$ , the system may vitrify at the glass transition temperature  $T_g$  when  $\tau_{S(\text{equ})}$  reaches  $\sim 100$  s (see Fig. 5). At any temperature below  $T_g$ , the system is trapped in the glassy state, and  $\eta$  is now controlled by the isostructural stress relaxation time  $\tau_{S(\text{iso})}$ , which notably diverges from  $\tau_{S(\text{equ})}$  (see Fig. 5). It is noteworthy to point out that  $\tau_{S(\text{iso})}$  is several orders of magnitude shorter than  $\tau_{S(\text{equ})}$  at temperatures below  $T_g$ . In other words, the viscosity of a glass is several orders of magnitude lower than that of the corresponding equilibrium liquid at the same temperature. Importantly, this difference is further exacerbated in hyperquenched glasses, where  $\tau_{S(\text{iso})}$  departs from  $\tau_{S(\text{equ})}$  at a higher temperature  $T_f$ . As shown by Moynihan *et al.*,<sup>38</sup> the greater the cooling rate, the greater the fictive temperature  $T_f$ . As per Eq. (4), it results that the isostructural viscosity controlling crystallization below  $T_g$  is many orders of magnitude lower than the equilibrium viscosity originally used to estimate  $I$  in Eq. (3). Therefore, to account for this divergence in viscosity at  $T_g$ , we use the Adam–Gibbs equation modified by Hodge<sup>39</sup> in Eq. (3). The results are shown in Fig. 6 for two glasses of fragility  $m = 40$  and  $m = 100$

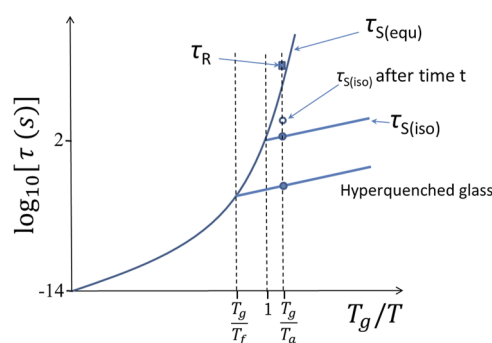


**FIG. 5.** Schematics of the temperature dependence of the relaxation time in a glass-forming liquid. The solid line corresponds to the equilibrium stress relaxation  $\tau_{S(\text{equ})}$ , whereas the dashed lines correspond to the isostructural stress relaxation time  $\tau_{S(\text{iso})}$  of the standard and hyperquenched glass.  $\tau_R$  is the structural relaxation time (enthalpy, volume, refractive index, etc.) measured without any applied stress. It represents the time that is needed for a glass to reach the equilibrium line.  $T_f$  is the fictive temperature of the hyperquenched glass, and  $T_a$  is the annealing temperature.



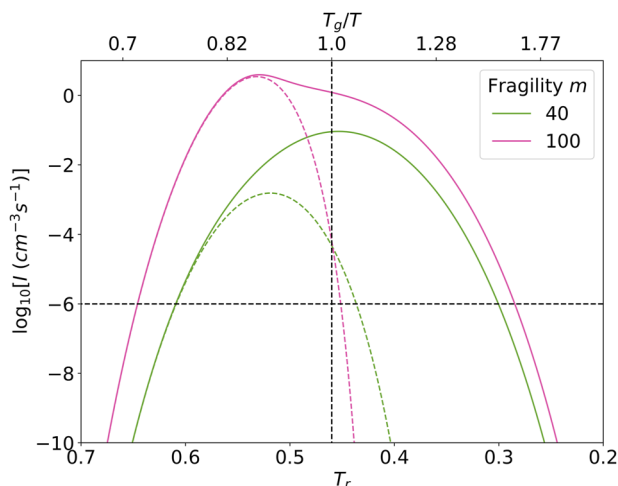


**FIG. 6.** Nucleation rate  $I$  computed using the Turnbull method modified with the Adam-Gibbs equation to account for the change of viscosity at and below  $T_g$ . Dotted lines are obtained using the equilibrium viscosity, whereas solid lines are obtained using the non-equilibrium isostructural viscosity in Eq. (3). Curves are shown for two glasses of fragility index  $m = 40$  and  $m = 100$  cooled at 10 000 K/s and with reduced glass temperature  $T_{rg} = 0.46$  corresponding to GeTe.

quenched at a rate of 10 000 K/s. Details of the calculation can be found in the Supplementary Information. Figure 6 shows that the nucleation rate  $I$  of the hyperquenched glassy state can be many orders of magnitude faster than that of the equilibrium liquid at and below  $T_g$ . This explains why some hyperquenched PCMs with a poor glass-forming ability such as GeTe ( $T_{rg} = 0.46$ ) can undergo fast crystallization even below the glass transition temperature. Other PCMs with a better glass-forming ability such as  $\text{Ge}_3\text{Sb}_6\text{Te}_5$  ( $T_{rg} = 0.56$ ) from Fig. 1 can exhibit a glass transition before crystallization, i.e., the nucleation curve would be shifted down to low values of  $I$  (see Fig. 4). The difference in crystallization behavior between these two systems can also be revealed through experimental measurement of their viscosity-temperature dependence, as shown in the following section titled “Fragile-to-strong transition.”

### Fragile-to-strong transition

The viscosity-temperature dependence of several PCMs is shown in Fig. 7 over nearly 16 orders of magnitudes. Viscosity measurements over such a broad range require multiple techniques including oscillating-cup viscometry, crystal growth velocity measurements from time-resolved reflectivity and transmission electron microscopy (TEM), as well as calorimetry. Experimental details about each method and the measurements on GeTe can be found in Ref. 20 and the method section, respectively. Several features are noteworthy in the viscosity-temperature dependence presented in Fig. 7. The first feature is a sudden change in fragility in the region  $T_g/T = 0.6\text{--}0.7$ . The liquids are initially strong at lower temperatures with a fragility index near  $m = 40$  and suddenly switch to a fragile behavior with a fragility index near  $m = 100$ . The full curve cannot be fitted with conventional models such as VFT or MYEGA<sup>40</sup> and, therefore, indicates a transition in fragility. This

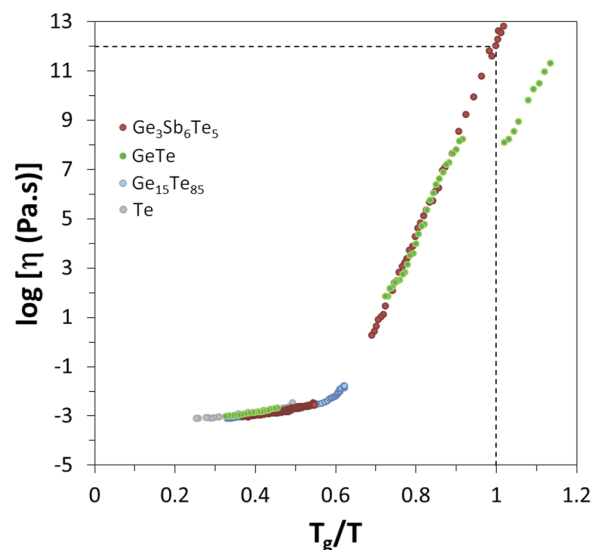


**FIG. 7.** Viscosity-temperature dependence of  $\text{Ge}_3\text{Sb}_6\text{Te}_5$ , GeTe,  $\text{Ge}_{15}\text{Te}_{85}$ ,<sup>44</sup> and Te.<sup>45</sup> Viscosity in the range of  $10^{-4}\text{--}10^{-1}$  Pa.s was measured by oscillating-cup viscometry,  $1\text{--}10^8$  Pa.s by time-resolved reflectivity, and  $10^8\text{--}10^{13}$  by *in situ* transmission electron microscopy. Data for  $\text{Ge}_3\text{Sb}_6\text{Te}_5$  are from Ref. 20, where a decoupling factor  $\xi = 0.91$  between viscosity and diffusivity was found below  $T_g$ . Data for GeTe were collected for this work using the same method as for  $\text{Ge}_3\text{Sb}_6\text{Te}_5$ . The same decoupling factor  $\xi = 0.91$  was used for GeTe. The time-resolved reflectivity data for GeTe exhibit greater noise due to occasional nucleation during the measurement that may affect the crystal growth velocity estimate.

fragile-to-strong transition (FST) appears to be a common feature of PCMs.<sup>20,41</sup>

Figure 6 compares the nucleation behavior of two systems with fragility index  $m = 40$  and  $m = 100$  analogous to those found on each side of the FST in the previous PCMs. Based on these results, the FST is of significant benefit for PCM technology as it provides a lower nucleation rate below  $T_g$  for increased stability of the memory cell and better data retention, while simultaneously providing higher nucleation rate at a higher temperature for faster switching speed and rapid computing.

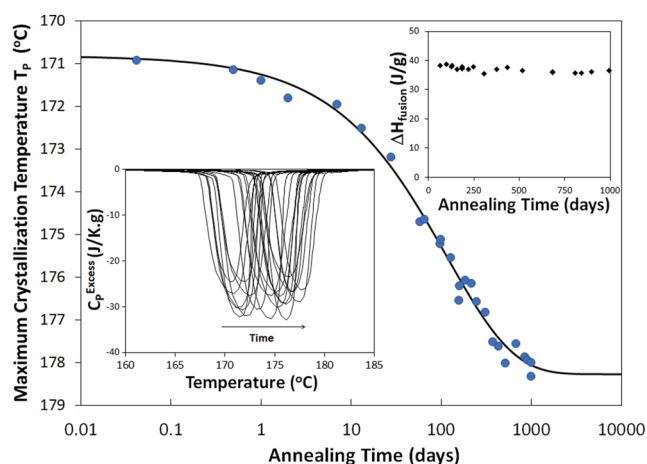
The second feature of interest in Fig. 7 is the mismatch in viscosity between GeTe and  $\text{Ge}_3\text{Sb}_6\text{Te}_5$  on approaching  $T_g$ . This pattern is reminiscent of the departure of  $\tau_{S(\text{iso})}$  from  $\tau_{S(\text{equ})}$  in Fig. 5. In fact,  $\text{Ge}_3\text{Sb}_6\text{Te}_5$  is a relatively good glass-former, and all viscosity measurements are performed in the equilibrium supercooled liquid state down to  $T_g$  and slightly below.<sup>20</sup> The system then exhibits the expected viscosity  $\eta = 10^{12}$  Pa.s at  $T_g$ . No viscosity measurements were then performed in the glassy state for  $\text{Ge}_3\text{Sb}_6\text{Te}_5$ . In contrast, measurements performed on GeTe, at and below  $T_g$ , show much lower viscosity than expected from equilibrium. This departure from equilibrium is consistent with measurements of isostructural viscosity in the glassy state.<sup>42,43</sup> Although these measurements unambiguously show that the system is trapped in a non-equilibrium state, the absolute value of viscosity should be subject to significant caveat. This is because the measurements take a certain amount of time during which the system may undergo

structural relaxation, as depicted in Fig. 5, for an annealing temperature  $T_a$  near  $T_g$ . Hence, the measured viscosity may reflect an average value of an intermediate state between the original glass and a partially relaxed glass. Consequently, the viscosity data measured in the glassy phase does not reflect the isostructural viscosity of the glassy phase; thus, a physically meaningful activation energy cannot be obtained. The effect of structural relaxation on the crystallization kinetics from the glassy state will be discussed in the following section titled “Effect of structural relaxation on sub- $T_g$  crystallization.”

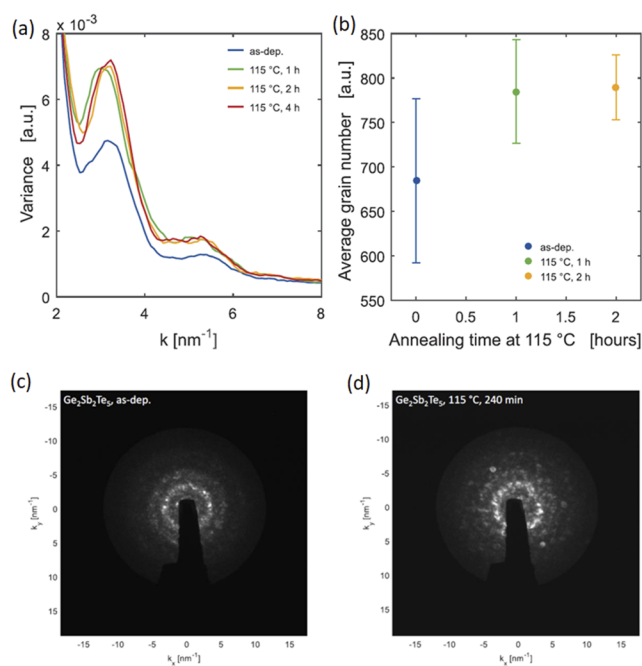
### Effect of structural relaxation on sub- $T_g$ crystallization

Figure 5 illustrates how  $\tau_{S(iso)}$ , given enough time, evolves toward  $\tau_{S(equ)}$  due to the natural tendency of glass to relax toward its equilibrium supercooled liquid state. The time constant  $\tau_R$  necessary for this process has been shown to be slightly longer than  $\tau_{S(equ)}$  and much longer than  $\tau_{S(iso)}$  (Fig. 5).<sup>42,46</sup> Therefore, the crystallization kinetics controlled by  $\tau_{S(iso)}$  in the glassy state should slowly evolve in a way consistent with the dynamics of structural glass relaxation controlled by  $\tau_R$ . Figure 8 shows how the maximum crystallization temperature  $T_p$  of a  $\text{Ge}_2\text{Sb}_2\text{Te}_5$  glass ( $T_g = 200^\circ\text{C}$ ) evolves over three years of annealing at  $75^\circ\text{C}$ . The shift in  $T_p$  follows a non-exponential decay function of the Kohlrausch–Williams–Watts (KWW)<sup>47,48</sup> form that is characteristic of glass relaxation.<sup>49</sup> The inset of Fig. 8 shows that the enthalpy of fusion is constant and that the system has not significantly crystallized during annealing. The increase in  $T_p$  indicates that crystallization is being delayed as a result of annealing and requires higher thermal energy. This increase in crystallization temperature is opposite to that expected if the system had nucleated during the annealing procedure. Yet, fluctuation electron microscopy (FEM) and TEM analysis of  $\text{Ge}_2\text{Sb}_2\text{Te}_5$  before and after annealing reveal an increase in a number of sub-

critical nuclei (see Fig. 9).<sup>14</sup> The FEM variance that is a measure of medium-range order and oftentimes interpreted as an increase in the sub-critical nuclei distribution increases during annealing, as shown in Fig. 9(a). After annealing, some nanodiffraction patterns taken for FEM reveal nanocrystalline diffraction spot, which were not found in the as-deposited (un-annealed) state, as shown in Figs. 9(c) and 9(d), indicating an increase in critical nuclei number. Finally, the number of grains obtained by TEM imaging following annealing at  $115^\circ\text{C}$  and crystallization at  $150^\circ\text{C}$  shows a significant increase because of the pre-annealing treatment, as shown in Fig. 9(b).<sup>14</sup> The presence of these subcritical nuclei should favor crystallization and lower the crystallization temperature, contrary to the shift observed experimentally in Fig. 8. Therefore, another more significant contribution must hinder crystallization during annealing. This contribution is the increase in isostructural viscosity  $\eta_{(iso)}$  expected from the relaxation process depicted in Fig. 5 and observed experimentally in amorphous chalcogenides.<sup>43</sup> An increase in viscosity is expected to lower both crystal growth and nucleation rate [Eq. (3)] and should, therefore, delay crystallization to a higher temperature during heating at a constant rate, as observed experimentally. This also means that the effect of increased viscosity due to glass aging outperforms the increase in nucleation tendency deduced from the rise in FEM variance during pre-annealing.



**FIG. 8.** Evolution of the maximum crystallization temperature  $T_p$  of a  $\text{Ge}_2\text{Sb}_2\text{Te}_5$  glass during annealing at  $75^\circ\text{C}$ . The lower left inset shows the upward shift of the crystallization exotherm as a function of annealing time. The upper right inset shows that the enthalpy of fusion remains mainly constant throughout the annealing procedure.



**FIG. 9.** (a) Fluctuation electron microscopy variance of a  $\text{Ge}_2\text{Sb}_2\text{Te}_5$  glass after annealing at  $115^\circ\text{C}$ . An increase in variance indicates an increase in medium-range order. (b) Average grain number obtained from TEM image analysis after annealing  $\text{Ge}_2\text{Sb}_2\text{Te}_5$  glass at  $115^\circ\text{C}$  following crystallization at  $150^\circ\text{C}$  for one hour. Nanodiffraction pattern collected (c) before annealing and (d) after annealing at  $115^\circ\text{C}$  showing an increase in nanocrystalline diffraction spots. Note that diffraction patterns showing nanocrystalline diffraction patterns are excluded from the FEM calculation in (a) in order to investigate the medium-range order change in the purely amorphous phase. Figures adapted from Ref. 14.

The non-exponential decay of  $T_p$  observed in Fig. 8 is characteristic of glass structure relaxation dynamics.<sup>50</sup> Dynamic heterogeneities intrinsic to glasses result in a distribution of relaxation times and a non-exponential relaxation process.<sup>51</sup> The fit shown in Fig. 8 yields a non-exponential factor  $\beta = 0.59$  and a characteristic relaxation time  $\tau = 116$  days ( $10^7$  s). This magnitude of relaxation time is consistent with that of structural relaxation in glass far below  $T_g$ . Overall, the results of Fig. 8 further support the conclusion that PCMs can crystallize from the glassy state when reheated at standard rates.

## DISCUSSION

Crystallization below the glass transition temperature  $T_g$  is not uncommon. In particular, organic glasses frequently exhibit unusually high crystallization rates below  $T_g$ .<sup>2–9</sup> These unexpectedly fast crystallizations are the result of decoupling between diffusivity and viscous flow, which is exacerbated by high fragility.<sup>52</sup> Nevertheless, these systems are fairly good glass-formers that exhibit a clear glass transition when measured at the standard rate of 20 °C/min. On the other end, very poor glass-formers that require hyperquenching to vitrify, such as PCMs, do not exhibit a calorimetric glass transition when reheated at standard rates. Although they also undergo a decoupling between diffusivity and viscous flow on approaching  $T_g$ , they are also subjected to very high fictive temperatures that considerably lower their isostructural viscosity. This low effective viscosity promotes both fast nucleation and fast crystal growth. As a consequence, they systematically crystallize prior to reaching  $T_g$  when reheated at standard rates.

The Turnbull parameter  $T_{rg}$  is generally reliable and has been broadly used in the glass community to assess glass-forming ability.<sup>53</sup> Consistent trends in the Turnbull parameter can be observed in PCMs, where compounds with low parameter values such as GeTe ( $T_{rg} = 0.46$ ) and  $\text{Ge}_2\text{Sb}_2\text{Te}_5$  ( $T_{rg} = 0.52$ ) are very poor glass-former without measurable calorimetric  $T_g$ , whereas compounds with higher parameter values such as  $\text{Ge}_3\text{Sb}_6\text{Te}_5$  ( $T_{rg} = 0.56$ ) and GeSe ( $T_{rg} = 0.58$ ) are better glass-former with a distinct glass transition endotherm. Nevertheless, some notable exception exists such as AIST ( $T_{rg} = 0.56$ ), which does not exhibit a glass transition at a standard heating rate despite its high Turnbull parameter.<sup>15</sup> This indicates that other contributions besides the thermodynamic factors governing the difference between  $T_g$  and  $T_m$  must play a significant role in controlling crystallization kinetics. In particular, it was recently shown that glass-formation and crystallization rates were strongly dependent on bonding characteristics in PCMs.<sup>19</sup>

Crystalline phase change materials such as GeTe,  $\text{Ge}_2\text{Sb}_2\text{Te}_5$ , and  $\text{Sb}_2\text{Te}_3$  are characterized by an unconventional bonding mechanism, which differs from ionic, metallic, and covalent bonding.<sup>54</sup> The bonding has been denoted as metavalent bonding (MVB). This bonding mechanism is characterized by an unconventional property portfolio including large chemical bond polarizability as evidenced by high values of the Born effective charge  $Z^*$  and high values of  $\epsilon_\infty$ , the optical dielectric constant.<sup>55,56</sup> MVB is also characterized by an unconventional bond rupture upon laser-assisted field evaporation.<sup>57</sup> Characteristic of this bonding mechanism is a competition between electron delocalization as in metallic bonding and electron

localization as in covalent or ionic bonding. As a consequence, interfacial energies between the undercooled liquid and the crystalline phase are quite low, despite the pronounced change in atomic arrangement.<sup>58</sup> MVB solids have a small electron transfer between atoms and share only about half an electron pair between adjacent atoms, unlike covalent solids, where about one electron pair is formed, e.g., diamond.<sup>59</sup> Hence, in a map, metavalent solids are located between metals and covalently bonded solids. Compounds such as GeTe, as well as  $\text{Sb}_2\text{Te}_3$ <sup>60</sup> and PbSe,<sup>61</sup> employ this bonding mechanism. The distinct nature of this bond is also supported by pronounced property changes upon the transition from metavalent to covalent bonding.

In the amorphous phase, where the bonding is supposed to be covalent, locally ordered regions averaging one shared electron per bond (about half an electron pair) such as fourfold rings are also believed to play a role in the fast crystallization kinetics of some systems.<sup>62,63</sup> Furthermore, the small interfacial energy at elevated temperatures helps to realize a high crystallization speed.<sup>58</sup> Meanwhile, the more pronounced Peierls distortion near and below  $T_g$  stabilizes the glassy phase.<sup>64</sup> Hence, multiple factors are at play in predicting crystallization speed and glass-forming ability. More systematic studies of thermodynamic, kinetic, and chemical bonding properties may reveal whether or not they are related to a common physical origin.

## CONCLUSION

Very poor glass-formers can only be vitrified through hyperquenching. They can be found across a broad category of materials including PCMs, some metallic alloys, and molecular liquids such as water. Interestingly, they share a common calorimetric feature in that they do not exhibit a glass transition endotherm prior to crystallization. Using the case of PCMs, this study has shown that these amorphous solids can crystallize below the glass transition. Evidence for this process includes the appearance of a glass transition endotherm at ultra-fast heating rates concomitant with a sudden change in crystallization kinetics as the system switches from crystallizing from the glassy to the liquid state. In addition, the pre- $T_g$  relaxation exotherm can only be rationalized if the  $T_g$  lays above the crystallization exotherm during a standard heating ramp. Moreover, the maximum crystallization temperature  $T_p$  is found to increase with annealing time despite the more abundant sub-critical nuclei that should speed up crystallization. This observation is not consistent with crystallization from the liquid state but is consistent with an increase in isostructural viscosity during the structural relaxation of the glass. This is confirmed by the non-exponential decay of the shift in  $T_p$  that is characteristic of the dynamic heterogeneity intrinsic to glasses. The characteristic time of 116 days associated with this process is also consistent with sub- $T_g$  structural relaxation. Finally, modeling based on the Turnbull equation shows that nucleation kinetics are, indeed, high even below  $T_g$  due to the hyperquenched nature of the system. This supports the ability of the system to undergo crystallization prior to the glass transition upon slow heating. The model also shows that the fragile-to-strong transition observed in PCMs is advantageous to slow down crystallization at low temperatures while increasing its speed at a higher temperature.



## EXPERIMENTAL SECTION

## Viscosity measurement

The viscosity of GeTe presented in Fig. 7 is determined from two types of crystal growth velocity measurements. On the one hand, samples prepared by magnetron sputter deposition were annealed isothermally in a differential scanning calorimeter (DSC) and the nucleated grains and their growth were investigated by transmission electron microscopy (TEM) for at least three times. Using the TEM method, the crystal growth velocity of the as-deposited phase is measured at temperatures from 135 °C up to 180 °C. For the highest treatment temperatures, the samples were dipped in a pre-heated oil bath and rapidly quenched in a room temperature bath of ethylene glycol, which allowed for annealing times on the timescale of seconds. The initially amorphous GeTe layer is 30 nm thick and encapsulated between two inert capping layers of (ZnS)<sub>80</sub>:(SiO<sub>2</sub>)<sub>20</sub>, which is supported by a Si<sub>3</sub>N<sub>4</sub> layer.

On the other hand, the crystal growth velocity is measured in a laser reflectivity setup. Here, the samples from the same magnetron deposition run were used in order to ensure the highest comparability between the measurement techniques. The samples were crystallized and brought to the temperature where the crystal growth velocity is supposed to be measured. Then, a laser pulse is used to melt-quench a 1.5 μm diameter spot to the amorphous phase, which induces a reflectivity change. Upon recrystallization of the melt-quenched amorphous spot, the reflectivity increases back to its original value. From this time-resolved reflectivity measurement, the crystal growth velocity is determined in the temperature range from 231.5 up to 365 °C. More information on both methods is reported in Ref. 20.

## Calorimetry

Enthalpy recovery exotherm for Ge<sub>2</sub>Sb<sub>2</sub>Te<sub>5</sub> and AIST in Fig. 2 and maximum crystallization temperature  $T_p$  of Ge<sub>2</sub>Sb<sub>2</sub>Te<sub>5</sub> in Fig. 8 were collected using a TA Q1000 DSC. A glass sample mass of 8–10 mg was sealed in an aluminum pan, and an empty pan was used as a reference. The temperature was calibrated with an indium standard, and the heat flow was calibrated with a sapphire standard. For the annealing procedure, 26 samples of Ge<sub>2</sub>Sb<sub>2</sub>Te<sub>5</sub> were sealed in an aluminum pan and introduced in an incubator at a temperature of 75 °C. Temperature stability was within 0.5 °C. At various time intervals, samples were removed from the incubator and allowed to cool down before being introduced in the DSC for measurement.

## SUPPLEMENTARY MATERIAL

See [supplementary material](#) for details of the numerical simulation of the nucleation rate in the equilibrium and at the non-equilibrium state.

## ACKNOWLEDGMENTS:

P.L. acknowledges financial support from NSF-DMR under Grant No. 1832817. J.P. and M.W. acknowledge funding in part from the Deutsche Forschungsgemeinschaft (DFG) via the collaborative research center Nanoswitches (Grant No. SFB 917) and in

part from the Federal Ministry of Education and Research (BMBF, Germany) in the project NEUROSYS (Grant No. 03ZU1106BA).

## AUTHOR DECLARATIONS

## Conflict of Interest

The authors have no conflicts to disclose.

## Author Contributions

**Pierre Lucas:** Funding acquisition (equal); Supervision (equal); Writing – original draft (lead). **Wataru Takeda:** Data curation (equal); Formal analysis (equal); Writing – review & editing (supporting). **Julian Pries:** Data curation (equal); Formal analysis (equal); Writing – review & editing (supporting). **Julia Benke-Jacob:** Data curation (equal); Formal analysis (equal). **Matthias Wuttig:** Funding acquisition (equal); Supervision (equal); Writing – review & editing (supporting).

## DATA AVAILABILITY

The data that support the findings of this study are available from the corresponding author upon reasonable request.

## REFERENCES

- 1 V. M. Fokin, A. S. Abyzov, N. S. Yuritsyn, J. W. P. Schmelzer, and E. D. Zanotto, “Effect of structural relaxation on crystal nucleation in glasses,” *Acta Mater.* **203**, 116472 (2021).
- 2 T. Hikima, Y. Adachi, M. Hanaya, and M. Oguni, “Determination of potentially homogeneous-nucleation-based crystallization in o-terphenyl and an interpretation of the nucleation-enhancement mechanism,” *Phys. Rev. B* **52**, 3900–3908 (1995).
- 3 H. Ishida, T. Wu, and L. Yu, “Sudden rise of crystal growth rate of nifedipine near  $T_g$  without and with polyvinylpyrrolidone,” *J. Pharm. Sci.* **96**, 1131–1138 (2007).
- 4 B. Schammé, X. Monnier, N. Couvrat, L. Delbreilh, V. Dupray, É. Dargent, and G. Coquerel, “Insights on the physical state reached by an active pharmaceutical ingredient upon high-energy milling,” *J. Phys. Chem. B* **121**, 5142–5150 (2017).
- 5 J.-F. Willart, L. Carpentier, F. Danède, and M. Descamps, “Solid-state vitrification of crystalline griseofulvin by mechanical milling,” *J. Pharm. Sci.* **101**, 1570–1577 (2012).
- 6 T. Wu and L. Yu, “Surface crystallization of indomethacin below  $T_g$ ,” *Pharm. Res.* **23**, 2350–2355 (2006).
- 7 L. Zhu, L. Wong, and L. Yu, “Surface-enhanced crystallization of amorphous nifedipine,” *Mol. Pharm.* **5**, 921–926 (2008).
- 8 Y. Sun, H. Xi, S. Chen, M. D. Ediger, and L. Yu, “Crystallization near glass transition: Transition from diffusion-controlled to diffusionless crystal growth studied with seven polymorphs,” *J. Phys. Chem. B* **112**, 5594–5601 (2008).
- 9 C. T. Powell, H. Xi, Y. Sun, E. Gunn, Y. Chen, M. D. Ediger, and L. Yu, “Fast crystal growth in o-terphenyl glasses: A possible role for fracture and surface mobility,” *J. Phys. Chem. B* **119**, 10124–10130 (2015).
- 10 Y. Yue and C. A. Angell, “Clarifying the glass-transition behaviour of water by comparison with hyperquenched inorganic glasses,” *Nature* **427**, 717–720 (2004).
- 11 V. Velikov, S. Borick, and C. A. Angell, “The glass transition of water, based on hyperquenching experiments,” *Science* **294**, 2335–2338 (2001).
- 12 M. J. Starink, “Analysis of aluminium based alloys by calorimetry: Quantitative analysis of reactions and reaction kinetics,” *Int. Mater. Rev.* **49**, 191–226 (2004).

- <sup>13</sup>M. A. B. Mendes, C. S. Kiminami, W. J. Botta Filho, C. Bolfarini, M. F. de Oliveira, and M. J. Kaufman, "Crystallization behavior of amorphous  $\text{Ti}_{51.1}\text{Cu}_{38.9}\text{Ni}_{10}$  alloy," *Mater. Res.* **18**, 104–108 (2015).
- <sup>14</sup>J. Pries, S. Wei, M. Wuttig, and P. Lucas, "Switching between crystallization from the glassy and the undercooled liquid phase in phase change material  $\text{Ge}_2\text{Sb}_2\text{Te}_5$ ," *Adv. Mater.* **31**, 1900784 (2019).
- <sup>15</sup>J. Pries, J. C. Sehringer, S. Wei, P. Lucas, and M. Wuttig, "Glass transition of the phase change material AIST and its impact on crystallization," *Mater. Sci. Semicond. Process.* **134**, 105990 (2021).
- <sup>16</sup>J. Pries, Y. Yu, P. Kerres, M. Häser, S. Steinberg, F. Gladisch, S. Wei, P. Lucas, and M. Wuttig, "Approaching the glass transition temperature of GeTe by crystallizing  $\text{Ge}_{15}\text{Te}_{85}$ ," *Phys. Status Solidi RRL* **15**, 2000478 (2021).
- <sup>17</sup>G. P. Johari, "Does water need a new  $T_g$ ?", *J. Chem. Phys.* **116**, 8067–8073 (2002).
- <sup>18</sup>P. Lucas, J. Pries, S. Wei, and M. Wuttig, "The glass transition of water, insight from phase change materials," *J. Non-Cryst. Solids: X* **14**, 100084 (2022).
- <sup>19</sup>C. Persch, M. J. Müller, A. Yadav, J. Pries, N. Honné, P. Kerres, S. Wei, H. Tanaka, P. Fantini, E. Varesi, F. Pellizzer, and M. Wuttig, "The potential of chemical bonding to design crystallization and vitrification kinetics," *Nat. Commun.* **12**, 4978 (2021).
- <sup>20</sup>J. Pries, H. Weber, J. Benke-Jacob, I. Kaban, S. Wei, M. Wuttig, and P. Lucas, "Fragile-to-strong transition in phase-change material  $\text{Ge}_3\text{Sb}_6\text{Te}_5$ ," *Adv. Funct. Mater.* **32**, 2202714 (2022).
- <sup>21</sup>Y. Yue, "Revealing the nature of glass by the hyperquenching-annealing-calorimetry approach," *J. Non-Cryst. Solids: X* **14**, 100099 (2022).
- <sup>22</sup>E. Morales-Sánchez, E. F. Prokhorov, A. Mendoza-Galván, and J. González-Hernández, "Determination of the glass transition and nucleation temperatures in  $\text{Ge}_2\text{Sb}_2\text{Te}_5$  sputtered films," *J. Appl. Phys.* **91**, 697–702 (2002).
- <sup>23</sup>J. A. Kalb, M. Wuttig, and F. Spaepen, "Calorimetric measurements of structural relaxation and glass transition temperatures in sputtered films of amorphous Te alloys used for phase change recording," *J. Mater. Res.* **22**, 748–754 (2007).
- <sup>24</sup>J. Orava, A. L. Greer, B. Gholipour, D. W. Hewak, and C. E. Smith, "Characterization of supercooled liquid  $\text{Ge}_2\text{Sb}_2\text{Te}_5$  and its crystallization by ultrafast-heating calorimetry," *Nat. Mater.* **11**, 279–283 (2012).
- <sup>25</sup>J.-Y. Cho, D. Kim, Y.-J. Park, T.-Y. Yang, Y.-Y. Lee, and Y.-C. Joo, "The phase-change kinetics of amorphous  $\text{Ge}_2\text{Sb}_2\text{Te}_5$  and device characteristics investigated by thin-film mechanics," *Acta Mater.* **94**, 143–151 (2015).
- <sup>26</sup>A. Sebastian, M. Le Gallo, and D. Krebs, "Crystal growth within a phase change memory cell," *Nat. Commun.* **5**, 4314 (2014).
- <sup>27</sup>J. Orava, D. W. Hewak, and A. L. Greer, "Fragile-to-strong crossover in supercooled liquid Ag-In-Sb-Te studied by ultrafast calorimetry," *Adv. Funct. Mater.* **25**, 4851–4858 (2015).
- <sup>28</sup>V. Velikov, S. Borick, and C. A. Angell, "Molecular glasses with high fictive temperatures for energy landscape evaluations," *J. Phys. Chem. B* **106**, 1069–1080 (2002).
- <sup>29</sup>H. S. Chen and E. Coleman, "Structure relaxation spectrum of metallic glasses," *Appl. Phys. Lett.* **28**, 245–247 (1976).
- <sup>30</sup>L. Hu, C. Zhang, and Y. Yue, "Structural evolution during the sub- $T_g$  relaxation of hyperquenched metallic glasses," *Appl. Phys. Lett.* **96**, 221908 (2010).
- <sup>31</sup>Y. Z. Yue, S. L. Jensen, and J. deC. Christiansen, "Physical aging in a hyperquenched glass," *Appl. Phys. Lett.* **81**, 2983–2985 (2002).
- <sup>32</sup>J. Huang and P. K. Gupta, "Enthalpy relaxation in thin glass fibers," *J. Non-Cryst. Solids* **151**, 175–181 (1992).
- <sup>33</sup>L. Hu and Y. Yue, "Secondary relaxation behavior in a strong glass," *J. Phys. Chem. B* **112**, 9053–9057 (2008).
- <sup>34</sup>D. W. Henderson, "Thermal analysis of non-isothermal crystallization kinetics in glass forming liquids," *J. Non-Cryst. Solids* **30**, 301–315 (1979).
- <sup>35</sup>H. E. Kissinger, "Reaction kinetics in differential thermal analysis," *Anal. Chem.* **29**, 1702–1706 (1957).
- <sup>36</sup>D. Turnbull, "Under what conditions can a glass be formed?," *Contemp. Phys.* **10**, 473–488 (1969).
- <sup>37</sup>M. Volmer and A. Weber, "Nucleus formation in supersaturated systems," *Z. Phys. Chem.* **119U**, 277–301 (1926).
- <sup>38</sup>C. T. Moynihan and P. B. Macedo, "Dependence of the glass transition temperature on heating rate and thermal history," *J. Phys. Chem.* **75**, 3379–3381 (1971).
- <sup>39</sup>I. M. Hodge, "Adam-Gibbs formulation of nonlinearity in glassy-state relaxations," *Macromolecules* **19**, 936–938 (1986).
- <sup>40</sup>J. C. Mauro, Y. Yue, A. J. Ellison, P. K. Gupta, and D. C. Allan, "Viscosity of glass-forming liquids," *Proc. Natl. Acad. Sci. U. S. A.* **106**, 19780–19784 (2009).
- <sup>41</sup>P. Zalden, F. Quirin, M. Schumacher, J. Siegel, S. Wei, A. Koc, M. Nicoul, M. Trigo, P. Andreasson, H. Enquist, M. J. Shu, T. Pardini, M. Chollet, D. Zhu, H. Lemke, I. Ronneberger, J. Larsson, A. M. Lindenberg, H. E. Fischer, S. Hau-Riege, D. A. Reis, R. Mazzarello, M. Wuttig, and K. Sokolowski-Tinten, "Femtosecond x-ray diffraction reveals a liquid-liquid phase transition in phase-change materials," *Science* **364**, 1062 (2019).
- <sup>42</sup>R. F. Lancelotti, D. R. Cassar, M. Nalin, O. Peitl, and E. D. Zanotto, "Is the structural relaxation of glasses controlled by equilibrium shear viscosity?," *J. Am. Ceram. Soc.* **104**, 2066–2076 (2021).
- <sup>43</sup>C. Bernard, G. Delaizir, J.-C. Sangleboeuf, V. Keryvin, P. Lucas, B. Bureau, X.-H. Zhang, and T. Rouxel, "Room temperature viscosity and delayed elasticity in infrared glass fiber," *J. Eur. Ceram. Soc.* **27**, 3253 (2007).
- <sup>44</sup>H. Weber, J. Orava, I. Kaban, J. Pries, and A. L. Greer, "Correlating ultrafast calorimetry, viscosity, and structural measurements in liquid GeTe and  $\text{Ge}_{15}\text{Te}_{85}$ ," *Phys. Rev. Mater.* **2**, 093405 (2018).
- <sup>45</sup>V. M. Glazov and O. D. Shchelikhov, "Change in short-range order structure in selenium and tellurium melts during heating," *Izv. Akad. Nauk SSSR, Neorg. Mater.* **10**, 202–207 (1974).
- <sup>46</sup>K. Doss, C. J. Wilkinson, Y. Yang, K. H. Lee, L. Huang, and J. C. Mauro, "Maxwell relaxation time for nonexponential  $\alpha$ -relaxation phenomena in glassy systems," *J. Am. Ceram. Soc.* **103**, 3590–3599 (2020).
- <sup>47</sup>R. Kohlrausch, "Theorie des elektrischen Rückstandes in der Leidener Flasche," *Ann. Phys. Chem.* **167**, 56–82 (1854).
- <sup>48</sup>G. Williams and D. C. Watts, "Non-symmetrical dielectric relaxation behaviour arising from a simple empirical decay function," *Trans. Faraday Soc.* **66**, 80–85 (1970).
- <sup>49</sup>C. T. Moynihan, "Structural relaxation and the glass transition," *Rev. Mineral.* **32**, 1–19 (1995).
- <sup>50</sup>R. Böhmer, K. L. Ngai, C. A. Angell, and D. J. Plazek, "Nonexponential relaxations in strong and fragile glass formers," *J. Chem. Phys.* **99**, 4201–4209 (1993).
- <sup>51</sup>M. D. Ediger, C. A. Angell, and S. R. Nagel, "Supercooled liquids and glasses," *J. Phys. Chem.* **100**, 13200–13212 (1996).
- <sup>52</sup>M. D. Ediger, P. Harrowell, and L. Yu, "Crystal growth kinetics exhibit a fragility-dependent decoupling from viscosity," *J. Chem. Phys.* **128**, 034709 (2008).
- <sup>53</sup>M. L. F. Nascimento, L. A. Souza, E. B. Ferreira, and E. D. Zanotto, "Can glass stability parameters infer glass forming ability?," *J. Non-Cryst. Solids* **351**, 3296–3308 (2005).
- <sup>54</sup>B. J. Kooi and M. Wuttig, "Chalcogenides by design: Functionality through metavalent bonding and confinement," *Adv. Mater.* **32**, 1908302 (2020).
- <sup>55</sup>M. Wuttig, V. L. Deringer, X. Gonze, C. Bichara, and J.-Y. Raty, "Incipient metals: Functional MATERIALS with a unique bonding mechanism," *Adv. Mater.* **30**, 1803777 (2018).
- <sup>56</sup>C.-F. Schön, S. van Bergerem, C. Mattes, A. Yadav, M. Grohe, L. Kobbelt, and M. Wuttig, "Classification of properties and their relation to chemical bonding: Essential steps towards the inverse design of materials with tailored functionalities," *Sci. Adv.* **8**, eade0828 (2022).
- <sup>57</sup>M. Zhu, O. Cojocar-Mirédin, A. M. Mio, J. Keutgen, M. Küpers, Y. Yu, J.-Y. Cho, R. Dronskowski, and M. Wuttig, "Unique bond breaking in crystalline phase change materials and the quest for metavalent bonding," *Adv. Mater.* **30**, 1706735 (2018).
- <sup>58</sup>J. A. Kalb, F. Spaepen, and M. Wuttig, "Kinetics of crystal nucleation in undercooled droplets of Sb- and Te-based alloys used for phase change recording," *J. Appl. Phys.* **98**, 054910 (2005).
- <sup>59</sup>J. Y. Raty, M. Schumacher, P. Golub, V. L. Deringer, C. Gatti, and M. Wuttig, "A quantum-mechanical map for bonding and properties in solids," *Adv. Mater.* **31**, 1806280 (2019).

- <sup>60</sup>Y. Cheng, O. Cojocaru-Mirédin, J. Keutgen, Y. Yu, M. Küpers, M. Schumacher, P. Golub, J. Y. Raty, R. Dronskowski, and M. Wuttig, "Understanding the structure and properties of Sesqui-chalcogenides (i.e.,  $V_2VI_3$  or  $Pn_2Ch_3$  (Pn = Pnictogen, Ch = Chalcogen) compounds) from a bonding perspective," *Adv. Mater.* **31**, 1904316 (2019).
- <sup>61</sup>S. Maier, S. Steinberg, Y. Cheng, C. F. Schön, M. Schumacher, R. Mazzarello, P. Golub, R. Nelson, O. Cojocaru-Mirédin, J. Y. Raty, and M. Wuttig, "Discovering electron-transfer-driven changes in chemical bonding in lead chalcogenides (PbX, where X = Te, Se, S, O)," *Adv. Mater.* **32**, 2005533 (2020).
- <sup>62</sup>J. Hegedüs and S. R. Elliott, "Microscopic origin of the fast crystallization ability of Ge-Sb-Te phase-change memory materials," *Nat. Mater.* **7**, 399–405 (2008).
- <sup>63</sup>T. Matsunaga, J. Akola, S. Kohara, T. Honma, K. Kobayashi, E. Ikenaga, R. O. Jones, N. Yamada, M. Takata, and R. Kojima, "From local structure to nanosecond recrystallization dynamics in AgInSbTe phase-change materials," *Nat. Mater.* **10**, 129–134 (2011).
- <sup>64</sup>J. Y. Raty, W. Zhang, J. Lucas, C. Chen, R. Mazzarello, C. Bichara, and M. Wuttig, "Aging mechanisms in amorphous phase-change materials," *Nat. Commun.* **6**, 7467 (2015).